ISSN 1330-3651(Print), ISSN 1848-6339 (Online)
DOI: 10.17559/TV-20151026154842

DYNAMICS ANALYSIS AND ACTIVE CONTROL OF A FLOATING CRANE

Yougang Sun, Wanli Li, Dashan Dong, Xiao Mei, Haiyan Qiang

Original scientific paper

The floating cranes, which transfer payloads during offshore constructions, need meet rigorous demands for efficiency and safety in serious sea conditions while the unexpected motion of the floating crane caused by wave make it even harder. This paper analyses the dynamics of a floating crane and presents an active heave compensation system (HCS) to allow the payloads motion decoupled from the wave-induced ship motion in the vertical direction. Specifically, virtual prototyping technology is introduced for the floating crane systems to investigate the real behaviour of the HCS. A virtual mechanical model of the floating crane is created to analyse the dynamics of the floating crane. In addition, an active HCS is designed for the under actuated floating crane system. A self-adaptive PID control law based on improved genetic algorithm is proposed for the essential part of the HCS. The co-simulation and experiment results demonstrate that the payload motion due to the ship's vertical motion can be reduced significantly in harsh sea conditions.

Keywords: *floating crane; heave compensation; nonlinear control; offshore operation; virtual prototype*

Analiza dinamike i aktivno upravljanje ploveće dizalice

Izvorni znanstveni članak

Ploveće dizalice, koje prenose koristan teret tijekom izvođenja radova na otvorenom moru, moraju zadovoljiti rigorozne zahtjeve u pogledu učinkovitosti i sigurnosti u teškim uvjetima, dok ih iznenadno gibanje ploveće dizalice prouzročeno valovima, čini još težim. U radu se analizira dinamika ploveće dizalice i upoznaje s aktivnim sustavom za kompenzaciju dizanja i spuštanja broda (heave compensation system - HCS) s kojim se postiže pomicanje tereta nezavisno od gibanja broda prouzročenog valovima u uspravnom smjeru. Točnije, uvodi se virtualna tehnologija stvaranja prototipa za sustave plovećih dizalica s ciljem istraživanja stvarnog djelovanja HCS-a. Stvoren je virtualni mehanički model ploveće dizalice kako bi se analizirala dinamika dizalice. Uz to, konstruiran je aktivni HCS za potpogonjeni sustav ploveće dizalice. Za bitan dio HCS-a predlaže se zakon samopodesivog PID upravljanja zasnovan na poboljšanom genetskom algoritmu. Zajednička simulacija i eksperimentalni rezultati pokazuju da se pomicanje tereta zbog vertikalnog gibanja broda može značajno smanjiti u teškim morskim uvjetima.

Ključne riječi: *kompenzacija dizanja i spuštanja broda; nelinearno upravljanje; ploveća dizalica; rad na otvorenom moru; virtualni prototip*

1 Introduction

With the increasing demands for the exploitation of ocean resources, there will be more and more offshore constructions，such as offshore wind farm, oil and gas fields, offshore airport or cross-sea Bridge. Similar as onshore constructions, the safety and efficiency of offshore constructions are often affected by disoperations, accident collisions and so on. Nevertheless, in addition to these factors, main threat of the offshore constructions in terms of safety and efficiency is the harsh and changeable sea condition, which can be regarded as a persistent external disturbance.

Floating crane, which can transfer payloads from one ship to another, is widely used for the construction or maintenance of the offshore installations. A suspended load in the ship-mounted crane can be easily influenced by waves, wind and ocean currents which would produce complicated nonlinear dynamic responses and cause accidents. In fact, many transfer missions have to be suspended in the poor sea conditions to avoid collisions between loads and the deck of vessel, which will extend the time of project and increase costs. Therefore, it is a new challenge for the floating crane to do these offshore operations with higher efficiency, more safety and lower costs under harsh sea environment.

The main reason for the challenge is that the ships, on which the cranes are fixed, are easily caused to move away from the designated position horizontally and vertically. A dynamic positioning system and an anti-sway device are often employed to control the horizontal motion of the ship and the sway of the payloads separately. A lot of dynamic positioning systems have been presented based on linear or nonlinear control theories [1-3]. Meanwhile, numerous control strategies have been proposed to control the swaying of the suspended payload by a number of publications. For example，refer to Ngo et al. [4], Park et al. [5], Masoudet al. [6] and Fang et al. [7]. Nevertheless, in these literatures, the ship's vertical (heave) motion has not been paid enough attention. But for offshore load transfer operations, the heave motion of the ship holds great significance for the safety and efficiency of the floating crane system.

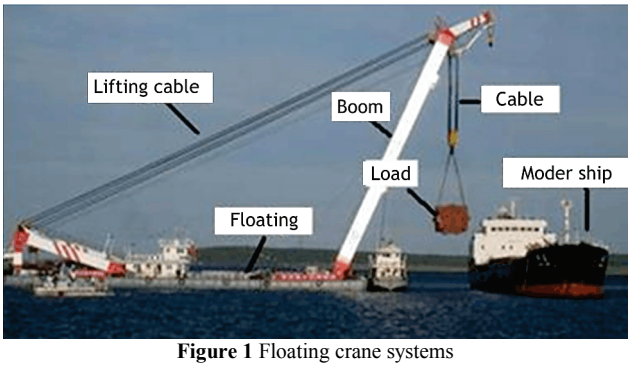

Figure 1 Floating crane systems

To ensure the high operability of the floating crane under harsh sea condition, the payload's vertical motion should be decoupled from the ship's heave movement, which can keep the lifting operations unaffected by the wind-induced or wave-induced ship's movement in the vertical direction. To achieve this goal, some researchers have started to investigate the heave compensation system (HCS), which is applied for remotely operated vehicle (ROV) [8], deep-water lifting [9, 10] and oil drilling ship

[11-13]. On the whole, there are three different ways for HCS. The first way is called passive heave compensation. Apart from utilizing follow-up hook system to detect the vertical motion between two ships for load transfer operations, pneumatic cylinders and an augment impedance control law were fused into a passive compensation system to compensate the heave movement for a drilling ship [14-16]. The second one is based on Semi-active heave compensation，which can achieve a balance between compensation precision and energy consumption [17]. The last approach is to design a completely active heave compensation system. Do et al. [12], for example, proposed an active heave compensation system for a rig using a nonlinear controller. The system utilized an electro-hydraulic system driven by a double rod actuator to reduce the effect of the vertical motion of the ship. Hatleskog et al. [13] presented an impedance approach with active heave compensation for resolving the bit-bounce, or contact-instability induced by ship heave. In [18], a disturbance decoupling controller with heave motion prediction is employed to control the hoisting winch of the crane to let the suspended payload track a desired trajectory. A similar problem is discussed in Kuchleret et al. [19]. They reduced the payload motion due to the ship's vertical motion efficiently by using an actuated oscillator together with a prediction algorithm. Additionally, some researchers have focused on control strategies to let the payload of a ship-mounted crane enter the water smoothly, which can refer to [20, 21].

In this paper, a dynamic model of the floating crane is derived and an active heave compensation system (HCS) is presented to control the payload descending at a desired speed relative to the vertical movement of ship's deck decoupled from the wave-induced ship motion. A novel controller is proposed to improve the robustness against the disturbances and system parameters variation. The HCS virtual model is built in the ADMAS, AMESim and MATLAB combined simulation environment to simulate real behaviour of the HCS under persistent sea wave disturbance. An experimental setup is established at last. Both co-simulation and experimental results are included to verify the efficiency of the designed HCS.

2 Dynamics development and analysis

Since working on the sea, the floating crane is affected by the wind and wave. Referring to Jang et al. [22], the wind-induced drag force in aerodynamics acting on the crane structures can be denoted as

$$F_D(t)=\frac{1}{2}\rho C_D A\overline{U}^2+\rho C_D A\overline{U}w(t)+\frac{1}{2}\rho C_D Aw(t)|w(t)| \quad (1)$$

where ρ and C_D represent air density and drag coefficient, respectively. A is utilized to denote the projected area of a structure. The $\overline{U}$ is a constant wind speed based on the height above the sea level, and $w(t)$ is utilized to represent the randomly fluctuating turbulent wind speed.

The last term of Eq. (1) is generally neglected. The second term of Eq. (1) is force related to a Gaussian random process with zero mean. The first term of Eq. (1) is constant for a given wind speed. In this paper, the floating crane height structures and projected area are teeny. Hence, the wind influence to the floating crane is regardless.

Furthermore, the wave is the main disturbance to the movement of the floating crane. The description of influence caused by the wave is imperative for modelling the dynamic of the floating crane. In order to analyse the nonlinear system, the wave force is split into two parts: the superposition of a harmonic force at the dominated frequency and a random disturbance [5]. We utilize $B\xi$ to represent the small random component f_α, ε and Ω are utilized to denote the amplitude, phase of wave, and frequency, respectively. The sea wave is denoted as follows:

$$s_w(t)=f_\alpha \sin(\Omega t+\varepsilon)+B\xi. \quad (2)$$

To model the floating crane system, we set up a moving coordinate attached to the ship besides an inertial frame of reference fixed on the ground. The moving frame I_M : $\{x_M\ y_M\ z_M\}$ is defined with the origin o_M fixed on the centre of the ship, the x_M - axis pointing to the fore, the y_M - axis parallel with deck. The coordinate system I_G : $\{x_G\ y_G\ z_G\}$ is fixed on the ground with the origin o_G fixed on the centre of the ship too. The points A, P and O denote the crane tip, the payload which is considered as a point mass, and the centre of the ship. In the moving frame of I_M, we utilize $(x_{C_M}\ y_{C_M}\ z_{C_M})$ to denote the ship's mass center.

For simplicity, we utilize S_α, C_α, S_β and C_β to represent the functions $\sin\alpha$, $\cos\alpha$, $\sin\beta$ and $\cos\beta$. According to coordinate relation, the point P of the payload is denoted in the frame of I_G as

$$\begin{bmatrix} x_{P_G} \\ y_{P_G} \\ z_{P_G} \end{bmatrix}=\begin{bmatrix} x_{A_G} \\ y_{A_G} \\ z_{A_G} \end{bmatrix}+\begin{bmatrix} LC_\alpha \\ LS_\alpha C_\beta \\ -LS_\alpha S_\beta \end{bmatrix}, \quad (2)$$

$$\begin{bmatrix} x_{A_G} \\ y_{A_G} \\ z_{A_G} \end{bmatrix}=\begin{bmatrix} x_{O_M} \\ y_{O_M} \\ z_{O_M} \end{bmatrix}+\boldsymbol{T}_O\begin{bmatrix} x_{A_M} \\ y_{A_M} \\ z_{A_M} \end{bmatrix}, \quad (4)$$

$$\boldsymbol{T}_O=\begin{bmatrix} 1 & -\psi & \theta \\ -\psi & 1 & -\varphi \\ -\theta & \varphi & 1 \end{bmatrix}, \quad (5)$$

where the matrix $\boldsymbol{T}_O\in\mathbb{R}^{3\times3}$ is utilized to depict the transition between the two frames of I_G and I_M, $L(t)$ is the length of cable.

A floating crane is a crane system mounted on a floating or a ship (Fig. 1). The movement of the load can be described by $2-D$ load's swing angles (α, β) and the cable length L. The signal of $u(t)\in\mathbb{R}^{6\times1}$ is utilized to represent the 6 DOFs of the ship of the floating crane (Fig. 2) the surge, sway, heave, roll, pitch and yaw, denoted as u = [x, y, z, φ, θ, ψ]. The velocity and acceleration are denoted as vectors $\dot{\boldsymbol{u}}(t)\in\mathbb{R}^{6\times1}$ and $\ddot{\boldsymbol{u}}(t)\in\mathbb{R}^{6\times1}$. We utilize the vector $\boldsymbol{F}(t)\in\mathbb{R}^{6\times1}$ to denote the forces and

the torques acted on the ship. The dynamics are obtained as follows:

$$\boldsymbol{M}\ddot{\boldsymbol{u}} = \boldsymbol{F}, \tag{6}$$

where, $\boldsymbol{M}$ is the generalized mass matrix of the ship assumed symmetrical to the longitudinal plane. The matrix $\boldsymbol{M}$ is explicitly defined in the following manner:

$$\boldsymbol{M} = \begin{bmatrix} m & 0 & 0 & 0 & mz_{C_M} & 0 \\ 0 & m & 0 & -mz_{C_M} & 0 & mx_{C_M} \\ 0 & 0 & m & 0 & -mx_{C_M} & 0 \\ 0 & -mz_{C_M} & 0 & I_4 & 0 & -I_{46} \\ mz_{C_M} & 0 & -mx_{C_M} & 0 & I_5 & 0 \\ 0 & mx_{C_M} & 0 & -I_{46} & 0 & I_6 \end{bmatrix},$$

where, m is the mass of the ship. I_4, I_5, I_6 are the moments of inertia of the x, y, z axis, respectively. I_{46} represents the product of inertia.

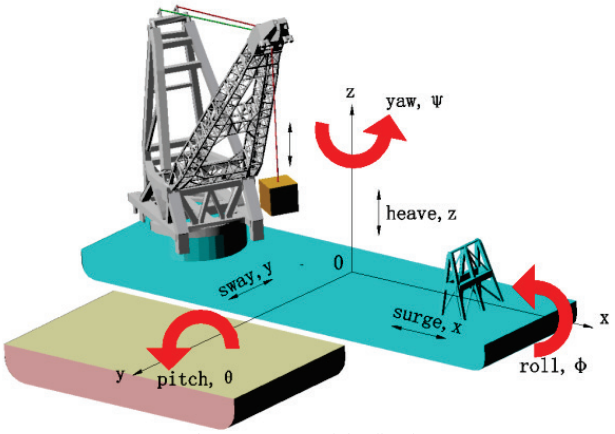

Figure 2 The movement of the floating crane

By utilizing Eq. (2) to get the derivation of time, the time-dependent relationship among the velocity and acceleration of the load, load's swing angles: $\alpha(t)$, $\beta(t)$ and the cable length $L(t)$ can be formed as

$$\dot{x}_{P_G} = \dot{x}_{A_G} + \dot{L}S_\alpha C_\beta + \dot{\alpha}LC_\alpha C_\beta - \dot{\beta}LS_\alpha S_\beta, \tag{7}$$

$$\dot{y}_{P_G} = \dot{y}_{A_G} - \dot{L}S_\beta - L\dot{\beta}C_\beta, \tag{8}$$

$$\dot{z}_{P_G} = \dot{z}_{A_G} + \dot{L}C_\alpha C_\beta - L\dot{\alpha}S_\alpha C_\beta - L\dot{\beta}C_\alpha S_\beta. \tag{9}$$

The generalized coordinate vector of the floating crane system is denoted as $\boldsymbol{V} = [x, y, z, \varphi, \psi, \alpha, \beta]^{\mathrm{T}}$ in the dynamic model. Yet there is only one control input of the winding drum control torque $M_W(t)$. Hence, the floating crane is a typical under actuated system.

3 The floating crane system model

3.1 Necessity of developing a virtual prototyping

For the development of a new control product, the traditional research methods require to build, test and verify on the hardware prototype, which takes up more time and cost. Especially for the large equipments like floating crane which has particular demands for the environment, most of the researchers do not have enough conditions to do physical model and then test. However, approach to overcome this problem. On the product of increasing complexity, the simulation technique based on the virtual prototype can significantly cut down manufacturing cost, reduce product development cycle and improve the market competition greatly.

The HCS for the floating crane is a typical hydromechatronic system. The design stages of mechanical, hydraulic and control are done with different software tools respectively but finally they should be integrated into a co-simulation prototyping. If there is a problem in the interaction operation among three systems, the designer must modify the mechanical design, hydraulic design and/or the control design to provide a perfect product.

3.2 Model of the mechanical system

In order to build the mechanical model of the floating crane system, all parts or components with the dimensions and shape of the physical model are modelled as 3D solid by SOLIDWORKS. These components were created with the geometric constraints displaying the characteristics of the floating crane system. Through applying the force and torque to drive the components of the floating crane model, this mechanical model evaluated and tested the "real" behaviour. It was then exported to ADAMS to execute the dynamic simulation.

In the ADAMS/view environment, a floating crane model is created as the following sequence. Firstly, the parameters of the components such as mass, material, density and inertia must be defined. Then by utilizing constraints, these parts are connected to each other. For example, the turntable is mounted on the ship using a revolute joint. The lifting cables are connected with boom using spherical joint. The end of lifting cable is fixed on the hoisting drum using a fixed joint. The ship is induced to sway and heave based on the wave disturbance function.

Especially, it is tough to generate the dynamic model of lifting cable winding the hoisting drum, since the cable should not only have the characteristics of the flexible body, but also realize inelastic elongation or shorten when lifting. Here some reasonable simplifications are made. An equivalent cable is utilized instead of the real way of cable winding the pulley block ignoring the friction. The cable is divided into small segments connected to each other with bushing forces. The cable winds the hoisting drum in order and contact forces between the hoisting drum and each discrete cable are added (Fig. 3). The real contact force of the objects can be equivalent to nonlinear spring-damper model based on penetration depth as follow:

$$F = \begin{cases} Max\left\{K\left(x_1 - x\right)^n - step\left(x, x_1 - d, C_{\max}, x_1, 0\right)\dot{x}, 0\right\} & x < x_1 \\ 0 & x > x_1 \end{cases} \tag{10}$$

where, K is the contact stiffness coefficient, x_1 is the displacement switch. x is the measured displacement variable. d is the penetration depth for the two contacted objects while the damper is the maximum. $C_{\max}$ is the

maximum contacting damper. $\dot{x}$ is the penetration depth. n is the stiffness force exponent.

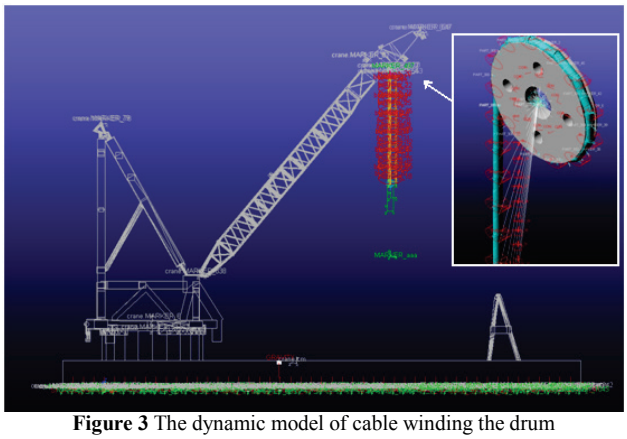

Figure 3 The dynamic model of cable winding the drum

Coulomb's friction model is adopted to define the tangential contact force between the cable and the hoisting drum.

$$f_t = -\mu(v_r) f_n \frac{v_r}{|v_r|}, \tag{11}$$

where f_n and μ are the normal contact force of the steel rope and the hoisting drum and the friction factor. v_r is the relative velocity of steel rope and hoisting drum.

The function relationship between friction factor μ and the relative velocity v_r is shown as follows:

$$\mu(v_r) = \begin{cases} \mu_s \left(\frac{v_r}{v_s}\right)^2 \left(3 - 2\frac{v_r}{v_s}\right) \operatorname{sgn}(-v_r) \\ \mu_s + (\mu_d - \eta_s)\left(\frac{v_r - v_s}{v_d - v_s}\right)^2 \left[3 - 2\left(\frac{v_r - v_s}{v_d - v_s}\right)\right] \operatorname{sgn}(-v_r) \\ \mu_d \operatorname{sgn}(-v_r) \end{cases} \tag{12}$$

where μ_s and μ_d are the static friction factors and the sliding friction factors. v_s and v_d are the static critical velocity and the sliding critical velocity.

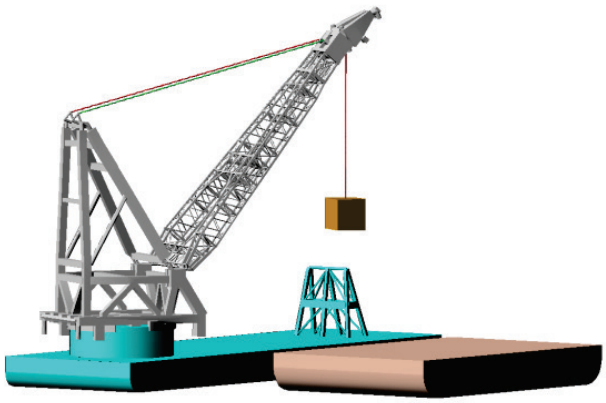

Figure 4 The mechanical system of the floating crane

The dynamic model of the floating crane has been built and is shown in Fig. 4. We can obtain dynamic response of the floating crane's hoisting system of different situation by modifying the parameter values used in the simulation. For example, at the level 3 sea conditions with 9,3 seconds wave period, 1,2 meters wave height, the cable is 22 meters, which is the resonant length. The suspended load's swing angles (α, β) can be depicted in Fig. 5.

The swing regulation and amplitude of the angles α and β are close to the results of [6, 23]. The validity of the model is verified in a 1/24-scale model of a crane ship through a motion platform of 3 DOFsin [23].

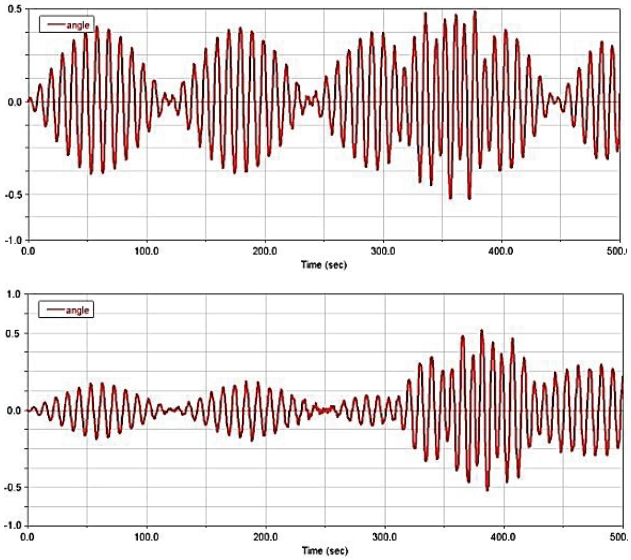

Figure 5 The load's swing angles (α, β)

The external environment and the parameter values can be modified to do some simulations which are high risk and low feasibility in real experiments. For example, at the level 5 sea conditions with 13,9 seconds wave period, 3 meters wave height, the falling speed of the loads is 8 m/min, and the resonance length is included in the range of changeable cable length when the loads descend to the ship. The distance change in the vertical direction between the falling load and the deck of moving ship is obtained in Fig. 6 by simulating two cases of different-phase of wave.

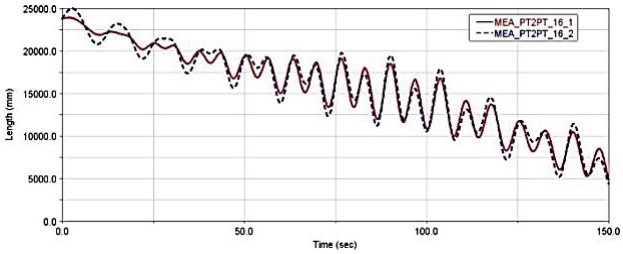

Figure 6 The vertical direction between the falling load and the deck (the red solid and blue dashed lines denote two cases of different-phase of wave, respectively)

Therefore, the ADAMS model can be used to simulate, test, analyze, and validate the characteristics of the floating crane mechanical model. Moreover, the model can be used to facilitate the control system design.

4 Control strategy design for the HCS

For a floating crane, we will design a heave compensation system (HCS) to control the payload descending at a desired speed relative to the vertical movement of ship's deck. That is, the payload must move at the assigned reference speed decoupled from the wave-induced ship motion. Based on the ADAMS dynamic model, the model of HCS is constructed in the AMESim environment which is well-known for designing a hydraulic control system. A feedback control law is constructed for the closed-loop system. The simulation results are collected to demonstrate the performance of the HCS of the floating crane.

4.1 Creating a HCS model

The structure of the control system for the heave compensation system is shown in Fig. 7. Input velocity is compared with actual detected velocity by servo-system, which would get the error signal of velocity. The error signal passes through controller and amplification to realize real-time control of servo valve to control velocity and direction of the load.

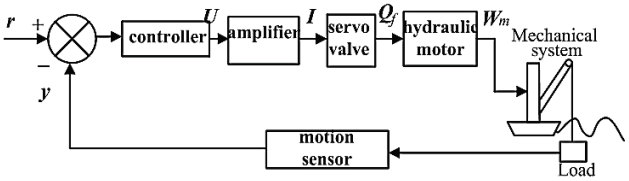

Figure 7 The structure of the control system

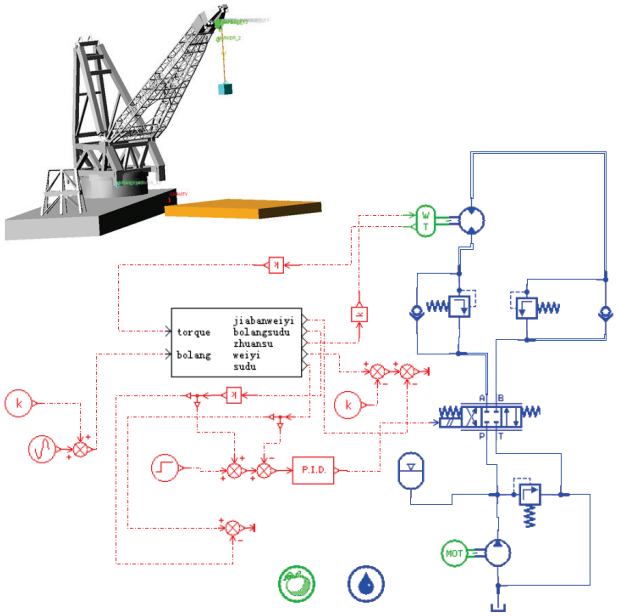

Figure 8 The HCS virtual model of the floating crane in the co-simulation environment

The flow continuity equation of servo valve to the hydraulic motor takes the following form:

$$Q_f = D_m\dot{\theta}_m + \frac{V_t}{4\beta_e}\dot{p}_f + C_{s1}p_f. \tag{13}$$

In analysis of the torque transmission, a torque balance equation can be formulated as

$$D_m p_f = J_1\ddot{\theta}_m + B_t\dot{\theta}_m + T_w, \tag{14}$$

where, p_f is the load pressure. D_m and θ_m represent the displacement and angle of hydraulic motor. J_1 denotes the rotational inertia of the hydraulic motor shaft, T_w is the output torque. B_t is a viscous damping coefficient.

Without tedious mathematical modelling, the AMESim provides users with graphical model of the hydraulic system, control system. Fig. 8 shows the HCS virtual model of the floating crane in the co-simulation of ADAMS and AMESim.

4.2 Control strategy design

As analyzed above, the floating crane model is a nonlinear system with persistent disturbance in the sea environment. The control goal of the HCS is to keep the payload descending at a desired speed in the vertical direction relative to the movement of ship's deck. The fluctuation of speed should be small. The conventional proportional-integral-derivative (PID) controller, which is linear combination of proportion, integration, differentiation, is expressed as the following:

$$u(t) = k_p\left[e(t) + \frac{1}{t_i}\int_0^t e(t)\mathrm{d}t + t_d\dot{e}(t)\right]. \tag{15}$$

A traditional PID control parameters tuning by trial-and-error method is widely applied in engineering. It has a high dependence on engineering experience, and does not always achieve optimal performance. For the HCS of floating crane, due to the different sea conditions, the parameters tuning in one sea condition may not work properly in another sea condition. If the overshoot is over, it will affect the work safety of the floating crane.

This paper presents an adaptive genetic algorithm (GA) PID controller, which combines the advantages of PID and GA, to achieve system robustness against parameter variations.

4.2.1 Online tuning process of genetic algorithm (GA)

GA is a random search method based on the biological laws of evolution. It can be applied widely in self-adaptive control field with the advantages of excellent optimization features, intelligence parameter tuning and fast speed without complex rules, which avoids finishing extensive knowledge base and a lot of simulations, experiments in expert control system for PID.

Since the PID controller has three parameters to be optimized, using real-coded multi-parameter in encoding genetic algorithm it combines the three real-coded parameters as a chromosome. The parameters are defined as $k_p(p_{\min}, p_{\max})$, $k_i(i_{\min}, i_{\max})$ and $k_d(d_{\min}, d_{\max})$. Chromosomes are composed by a code string in the form of three real numbers k_p, k_i and k_d. During decoding, cutting the code string can obtain the corresponding real numbers. The weighted sums of the error, the absolute

value of the error rate and integral absolute error are used as a minimum objective function. Moreover, a punitive function is employed, that is when $e(i) < 0$, the minimum objective function will add a term more than zero. Entire process of online optimization can be depicted as follows:

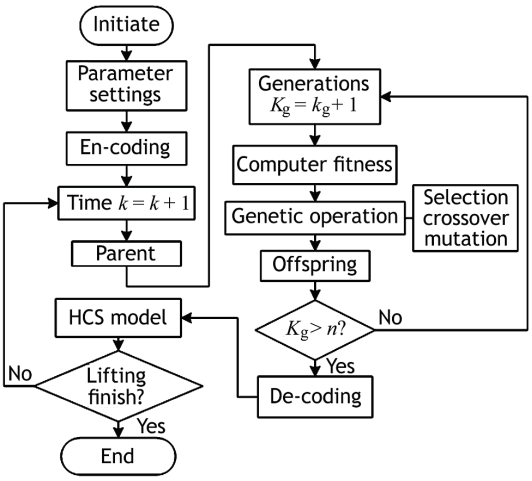

Figure 9 The process of online optimization based on GA

4.2.2 Improvement of genetic algorithm (GA)

GA is employed to design the controller of the HCS of the floating crane, which needs high efficiency to meet the real-time requirements. Moreover, to avoid invalid cross and in breeding, some improvements have been done in the genetic manipulation as follows:

(1) Change the sequential organization of the genetic manipulation and make the cross-operation and the copy-operation exist simultaneously. Set individual fitness value of parent population as $f(i)$ so that the selection probability should be:

$$p_s = \frac{f(i)}{\sum_{i=1}^{n} f(i)}, \tag{16}$$

where, the size of the population is n, the individual copy number is $m = p_s \cdot n$. If $m < 1$, set $m = 0$ and

$$nr = \left(n - \Sigma m\right) > 0.$$

(2) Change completely random characteristic of the crossover operation to make it selective. Introduce family index number to the individual. Forbid crossover operation with the same index number, shown in Fig. 10 (rs_i means family index number).

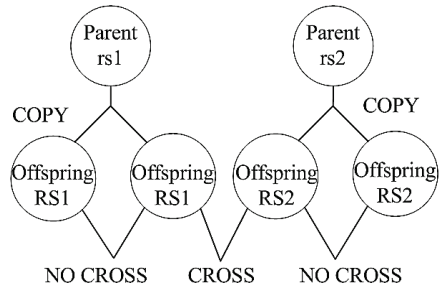

Figure 10 A selective crossover operation

The crossover operators of individuals i and j have the following form:

$$\begin{cases} X_i^{k+1} = \alpha X_i^k + (1-\alpha) X_j^k \\ X_j^{k+1} = (1-\alpha) X_i^k + \alpha X_j^k \end{cases}, \tag{17}$$

where, X_i^k, X_j^k are individuals of i, j, in the parent generation, while X_i^{k+1}, X_j^{k+1} are in the offspring, α means a random number between (0, 1).

(3) Change the random mutation to controlled random operations. Sequence individuals in the population from small to large according to fitness value, i_s denotes the serial number of individual i that the mutation probability can be obtained as follows

$$p_m = A - \frac{\delta \cdot i_s}{n}, \tag{18}$$

where, A is a constant to limit the maximum mutation probability, δ is the control factor less than 1, n is the size of the population.

4.3 Simulation results

The simulation is implemented in the HCS virtual model in the ADMAS, AMESim and MATLAB combined simulation environment. The dynamic, hydraulic and control model derived in sections above is used to show the performance of the HCS of the floating crane under the condition of system parameters variation and sea wave disturbance. The wave disturbances are varied by the frequency and height of the wave. The values of simulation parameters are shown in Tab. 1.

Table 1 The system parameters for simulation

Parameters	Values
Simulation time t	180 s
The control objectives: - Desired relative velocity v_z	 0,3 m/s
Model parameters: - Hydraulic system flow - Natural frequency of servo valve - Damping ratio of servo valve - Storage capacity of accumulator - Pressure of balance valve - Load mass	 1000 l/min 80 Hz 0,8 1000 l 20 bar 30 t
Disturbance parameters: - Sea wave height h_w - Sea wave frequency f_w	 0,5 m; 0,8 m 1,4 rad/s; 0,7 rad/s

The HCS should have perfect dynamic characteristics with quick response and small overshoot in any sea conditions. The conventional PID controller and the proposed controller are used to simulate under two different sea conditions. The step responses of the two controllers under two different sea conditions are shown in Fig. 11. The red and blue lines denote the step responses of the conventional PID and the proposed controllers in the first sea condition, respectively, while the purple and green lines depict the step responses of the two controllers respectively in the second sea condition.

As can be clearly seen from Fig. 11, the dynamic performance of the conventional PID is poor and the overshoot is quite big when the sea conditions change. Meanwhile, the proposed controller has an excellent performance with high speed of convergence, steady state error approximately zero, and the overshoots appear less than 2 % regardless of the sea conditions.

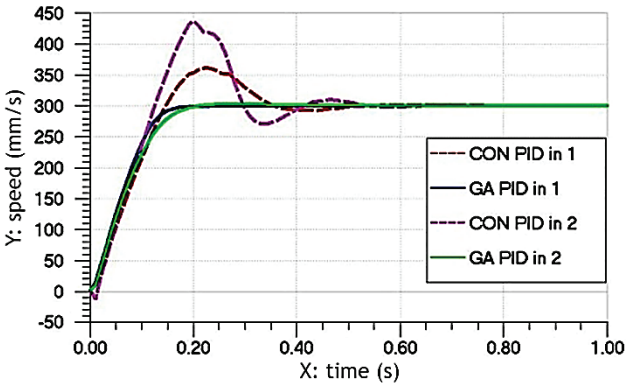

Figure 11 The step responses of the two controllers under two different sea conditions

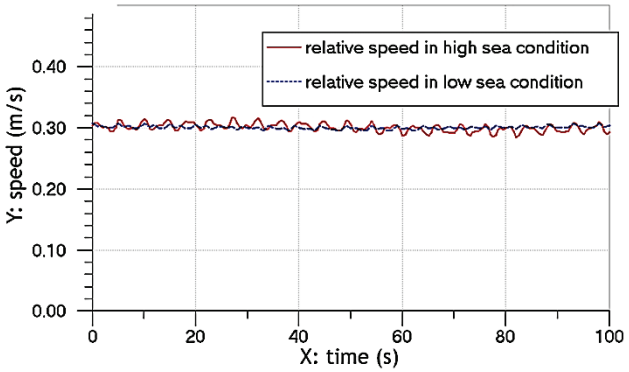

Figure 12 The relative speed in different sea conditions

Fig. 12 shows that the payload is always keeping in the speed of 0,3 m/s relative to the being supplied ship's deck vertical movement, which means the impact of the sea wave disturbance is reduced significantly. The co-simulation results are included to verify that the presented HCS can satisfy the control requirement for the floating crane in different sea conditions.

5 Experimental results

Since it is hard to build up a floating crane and test under disturbance from real sea waves, an experimental setup is built to further verify the performance of the control strategy of HCS. Experimental setup includes sensor test system, servo motor drive system, DSP control system and mechanical executive system shown in Fig. 14. Since it has made little difference to prove the effectiveness of control strategy of HCS, we choose servo motor as servo driver instead of hydraulic motor. One end of sensor is fixed on the payload and the other end is fixed on the simulation deck. The senor can measure the relative speed between the falling payload and simulation deck with up-and-down movement. Fig. 13 reveals the structure of the experimental system

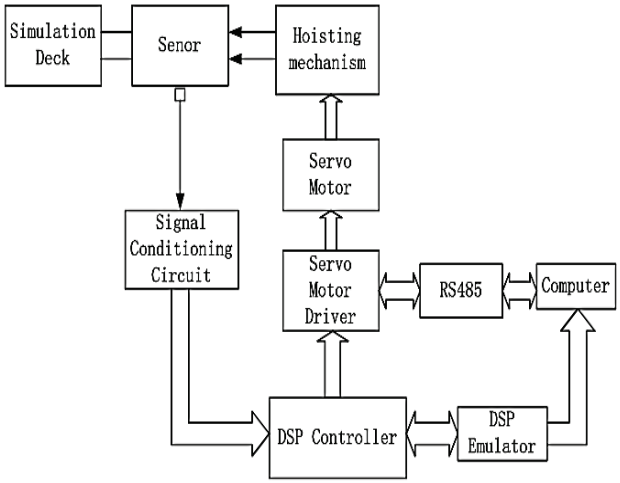

Figure 13 Structure of the experimental system

Set the system parameters as follows: the payload mass m_x = 10 kg the desired relative speed v_z = 3 cm/s low-frequency of deck movement $f_{lw} \approx 0{,}125$ Hz the high-frequency of deck movement $f_{hw} = 0{,}5$ Hz.

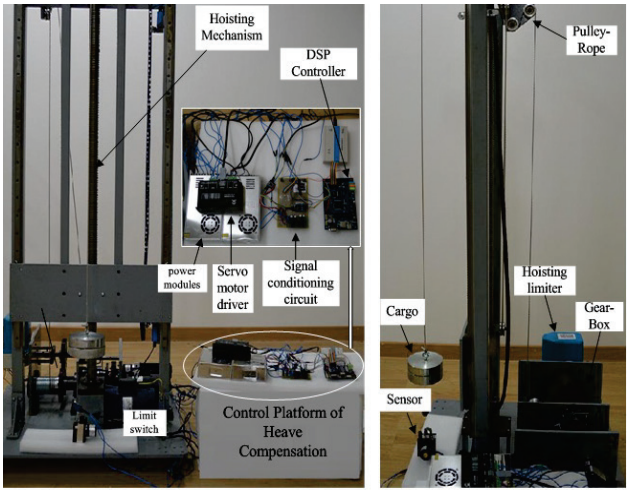

Figure 14 Experimental setup

Programme the online parameter tuning approach of PID based on GA in DSP controller. Improve the genetic operators of genetic algorithm to make the controller have higher search efficiency. Testing the improved GA by a six-hump camel back function, the evolution algebra is not more than 10 generations to reach the minimum value, while the traditional GA is about 30 generations.

The object of study is the relative speed between falling payload and moving deck in vertical direction. According to the experimental data recorded by DSP, draw the velocity change curve of falling payload and moving deck of different frequency interference, as shown in Fig. 15

It is shown in Fig. 15(a) that the active control system performed well with low frequency and the steady state error is less than 4 %, which is similar to the simulation results of the virtual prototype. Fig. 15 (b) shows that the frequency of forced vibration of the vessel would have great influence on the effect of compensation and the control properties while in the steady supplying condition. The payload vibrates slightly with high frequency, which reduces the precision of compensation. Since the frequency of the real sea wave is low, the proposed

control strategy for the HCS achieves the desired target. Both the simulation and experiment results prove that the HCS proposed in this paper is basically right and with excellent properties of speed tracking which can achieve the desired effect.

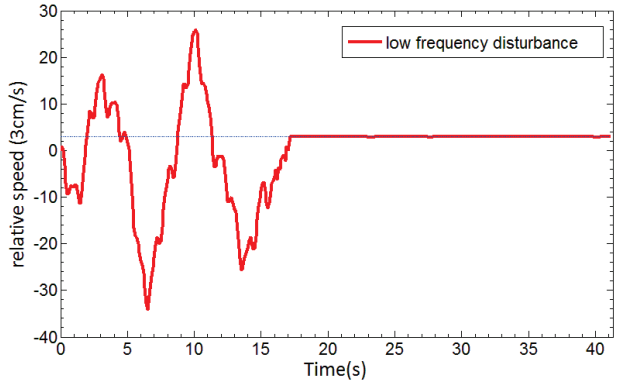

(a) Relative velocity of low-frequency disturbance

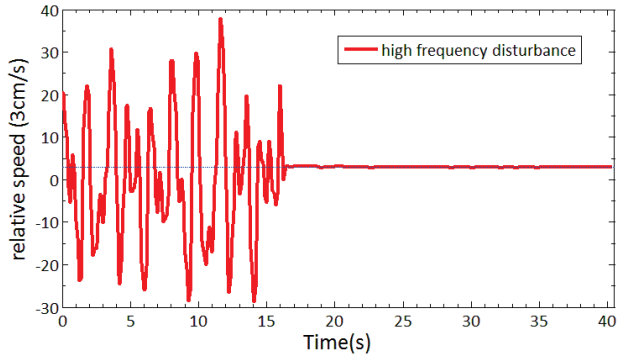

(b) Relative velocity of high-frequency disturbance

Figure 15 Experimental result of the relative payload speed. (From $t = 0$ *s*till $t = 16\ s$, the controller is switched off. From $t = 16\ s$ till $t = 41\ s$, the controller is switched on)

In summary, through the experimental results, the proposed HCS for the floating crane can be used effectively to control the payload descending at a desired speed decoupled from the vertical movement of ship's deck. Specially, the presented control approach utilizes the GA to online tuning the parameters of PID according to the varying wave disturbance, which improves the robustness against the disturbances and system parameters variation.

6 Conclusions

In this paper, the coupled dynamic model of the complex ship-crane-payload system was presented. Based on the model, an active heave compensation system (HCS) for offshore crane was presented to reject the disturbance of the sea wave efficiently by designing a novel nonlinear controller with brilliant performance. Through co-simulation and experimental results, the HCS for the floating crane was verified to track the change of the wave in time and make quick response to ensure the safety and efficiency in harsh sea conditions. Moreover, the integrative virtual prototype of mechanical, hydraulic and control model of the HCS can be described as a new approach for the marine engineering, which reduces manufacturing cost and time significantly. Our future work will apply the proposed HCS to actual floating crane systems.

Acknowledgements

This project is supported by Key Projects in the National Science & Technology Pillar Program of China (2013BAG19B00-01) and Key Projects in the National Science & Technology Pillar Program during the Twelfth Five-year Plan Period (2011BAJ02B00).

7 References

[1] Do, K. D.; Jiang, Z. P.; Pan, J. Universal controllers for stabilization and tracking of underactuated ships. // Systems & Control Letters. 47, 4(2002), pp. 299-317. DOI: 10.1016/S0167-6911(02)00214-1

[2] Liao, Y. L.; Su, Y. M.; Cao, J. Trajectory planning and tracking control for underactuated unmanned surface vessels. // Journal of Central South University. 21, 2(14), pp. 540-549.

[3] Serrano, M. E.; Scaglia, G. J. E.; Godoy, S. A. Trajectory Tracking of Underactuated Surface Vessels: A Linear Algebra Approach. // IEEE Transactions on Control Systems Technology. 22, 3(2014), pp. 1103-1111. DOI: 10.1109/TCST.2013.2271505

[4] Ngo, Q. H.; Hong, K. S. Sliding-Mode Antisway Control of an Offshore Container Crane. // Ieee-Asme Transactions on Mechatronics,17,2(2012), pp. 201-209. DOI: 10.1109/TMECH.2010.2093907

[5] Park, H. S.; Le, N. T. Modeling and Controlling the Mobile Harbour Crane System with Virtual Prototyping Technology. // International Journal of Control Automation and Systems. 10, 6(2012), pp. 1204-1214. DOI: 10.1007/s12555-012-0615-y

[6] Masoud, Z. N.; Nayfeh, A. H.; Mook, D. T. Cargo pendulation reduction of ship-mounted cranes. // Nonlinear Dynamics. 35, 3(2004), pp. 299-311. DOI: 10.1023/B:NODY.0000027917.37103.bc

[7] Fang, Y. C.; Wang, P. C.; Sun, N.; Zhang, Y. C. Dynamics Analysis and Nonlinear Control of an Offshore Boom Crane. // IEEE Transactions on Industrial Electronics. 61, 1(2014), pp. 414-427. DOI: 10.1109/TIE.2013.2251731

[8] Li, J. W.; Ge, T.; Wang, X. Y. Active Heave Compensation Control of ROVS. // Asian Journal of Control. 15, 2(2013), pp. 543-552. DOI: 10.1002/asjc.575

[9] Sagatun, S. I. Active control of underwater installation. // IEEE Transactions on Control Systems Technology. 10, 5(2002), pp. 743-748. DOI: 10.1109/TCST.2002.801783

[10] Nam, B. W.; Hong, S. Y.; Kim, Y. S.; Kim, J. W. Effects of Passive and Active Heave Compensators on Deepwater Lifting Operation. // International Journal of Offshore and Polar Engineering. 23, 1(2013), pp. 33-37.

[11] Korde, U. A. Active heave compensation on drill-ships in irregular waves. // Ocean Engineering. 25, 7(1998), pp. 541-561. DOI: 10.1016/S0029-8018(97)00028-0

[12] Do, K. D.; Pan, J. Nonlinear control of an active heave compensation system. // Ocean Engineering. 35, 5-6(2008), pp. 558-571. DOI: 10.1016/j.oceaneng.2007.11.005

[13] Hatleskog, J. T.; Dunnigan, M. W. An impedance approach to reduce the contact-instability whilst drilling with active heave compensation. // Ocean Engineering. 49, (2012), pp. 25-32. DOI: 10.1016/j.oceaneng.2012.04.001

[14] Hatleskog, J. T.; Dunnigan, M. W. Passive compensator load variation for deep-water drilling. // IEEE Journal of Oceanic Engineering. 32, 3(2007), pp. 593-602. DOI: 10.1109/JOE.2007.895276

[15] Driscoll, F. R.; Nahon, M.; Lueck, R. G. A comparison of ship-mounted and cage-mounted passive heave compensation systems. // Journal of Offshore Mechanics and Arctic Engineering-Transactions of the ASME. 122, 3(2000), pp. 214-221. DOI: 10.1115/1.1287167

[16] Hatleskog, J. T.; Dunnigan, M. W. Deepwater drilling using a passive compensator - Moderate heave conditions illustrate both load variation and contact-instability. // Sea Technology. 48, 4(2007), pp. 23-26.
[17] Huang, L. M.; Zhang, Y. T.; Zhang, L.; Liu, M. Y. Semi-active drilling drawworks heave compensation system. // Petroleum Exploration and Development. 40, 5(2013), pp. 665-670. DOI: 10.1016/S1876-3804(13)60089-0
[18] Neupert, J.; Mahl, T.; Haessig, B.; Sawodny, O.; Schneider, K. A heave compensation approach for offshore cranes. // 2008 American Control Conference/Washington, 2008, pp. 538-543. DOI: 10.1109/ACC.2008.4586547
[19] Kuchler, S.; Mahl, T.; Neupert, J.; Schneider, K.; Sawodny, O. Active Control for an Offshore Crane Using Prediction of the Vessel's Motion. // IEEE-ASME Transactions on Mechatronics. 16, 2(2011), pp. 297-309. DOI: 10.1109/TMECH.2010.2041933
[20] Johansen, T. A.; Fossen, T. I.; Sagatun, S. I.; Nielsen, F. G. Wave synchronizing crane control during water entry in offshore moonpool operations - Experimental results. // IEEE Journal of Oceanic Engineering. 28, 4(2003), pp. 720-728. DOI: 10.1109/JOE.2003.819155
[21] Skaare, B.; Egeland, O. Parallel force/position crane control in marine operations. // IEEE Journal of Oceanic Engineering. 31, 3(2006), pp. 599-613. DOI: 10.1109/JOE.2006.880394
[22] Jang, J. J.; Lee, C. S. Reliability analysis of maximum wind force for offshore structure design. // Proceedings Of the Twelfth (2002) International Offshore And Polar Engineering Conference /Kitakyushu, 2002, pp. 442-449.
[23] Idres, M. M.; Youssef, K. S.; Mook, D. T.; Nayfeh, A. H. A nonlinear 8-DOF coupled crane-ship dynamic model. // Collection of Technical Papers – AIAA/ASME/ASCE/AHS/ASC Structures, Structural Dynamics and Materials Conference / Norfolk, 2003, pp. 4187-4197.

Authors' addresses

Yougang Sun, Ph.D candidate
School of Mechanical Engineering,
Tongji University,
Logistics Engineering College,
Shanghai Maritime University,
No. 4800, Cao'an Highway,
Shanghai 201804, China
E-mail: 1989yoga@tongji.edu.cn

Wanli Li, prof, Ph.D
School of Mechanical Engineering,
Tongji University,
No.4800, Cao'an Highway,
Shanghai 201804, China
E-mail: cnlwl@tongji.edu.cn

Dashan Dong, prof, Ph.D
Logistics Engineering College,
Shanghai Maritime University,
No.1550, Haigang Avenue,
Shanghai 201306, China
E-mail: dsdong@shmtu.edu.cn

Xiao Mei, Assoc. Prof., Ph.D
Logistics Engineering College,
Shanghai Maritime University,
No.1550, Haigang Avenue,
Shanghai 201306, China
E-mail: xiaomei@shmtu.edu.cn

Haiyan Qiang *(Corresponding author)*
School of Mechanical Engineering, Tongji University,
No. 4800, Cao'an Highway, Shanghai 201804, China
Logistics Engineering College,
Shanghai Maritime University,
No. 1550, Haigang Avenue,
Shanghai 201306, China
E-mail: hyqiang@shmtu.edu.cn